Growth limiting conditions and denitrification govern extent and frequency of volume detachment of biofilms

Nicolas Derlon, Carole Coufort-Saudejaud, Isabelle Queinnec, Etienne Paul

Growth limiting conditions and denitrification govern extent and frequency of volume detachment of biofilms

Nicolas Derlon [a,b,c,*,1], Carole Coufort-Saudejaud [a,b,c,2], Isabelle Queinnec [d,e], Etienne Paul [a,b,c]

[a] Université de Toulouse, INSA, UPS, INP, LISBP, 135 Avenue de Rangueil, F-31077 Toulouse, France
[b] INRA, UMR792 Ingénierie des Systèmes Biologiques et des Procédés, F-31400 Toulouse, France
[c] CNRS, UMR5504, F-31400 Toulouse, France
[d] CNRS, LAAS, 7 Avenue du colonel Roche, F-31077 Toulouse, France
[e] Université de Toulouse, UPS, INSA, INP, ISAE, LAAS, F-31077 Toulouse, France

HIGHLIGHTS

▶ We investigated the biofilm physical structure and its detachment mechanisms.
▶ Anoxic conditions favor the formation of homogeneous biofilm structures.
▶ Detachment of large particles occurs for all biofilms and dominates biomass loss.
▶ An increasing roughness induces an increase in the size of detached particles.
▶ Biofilm models should consider discrete volume detachment of large particles.

ABSTRACT

This study aims at evaluating the mechanisms of biofilm detachment with regard of the physical properties of the biofilm. Biofilms were developed in Couette–Taylor reactor under controlled hydrodynamic conditions and under different environmental growth conditions. Five different conditions were tested and lead to the formation of two aerobic heterotrophic biofilms (aeHB1 and aeHB2), a mixed autotrophic and heterotrophic biofilm (MAHB) and two anoxic heterotrophic biofilms (anHB1 and anHB2). Biofilm detachment was evaluated by monitoring the size of the detached particles (using light-scattering) as well as the biofilm physical properties (using CCD camera and image analysis). Results indicate that volume erosion of large biofilm particles with size ranging from 50 to 500 μm dominated the biomass loss for all biofilms. Surface erosion of small particles with size lower than 20 μm dominates biofilm detachment in number. The extent of the volume detachment events was governed by the size of the biofilm surface heterogeneities (i.e., the absolute biofilm roughness) but never impacted more than 80% of the mean biofilm thickness due to the highly cohesive basal layer. Anoxic biofilms were smoother and thinner than aerobic biofilms and thus associated with the detachment of smaller particles. Our results contradict the simplifying assumption of surface detachment that is considered in many biofilm models and suggest that discrete volume events should be considered.

1. Introduction

Detachment is a key process in biofilm systems that influences pathogen spreading [1], release of particles that have detrimental effects on production systems and/or on water quality [2], the extent of biofouling [3] or also system performances [4]. But the mechanisms of biofilm detachment are not well understood and still need to be evaluated for further improved modeling of biofilm systems [5]. To what extent are different physical structures of biofilms associated with similar detachment mechanisms is not clear. Detachment process also governs the distribution of the Solid Residence Time (SRT), which controls the growth of slow-growing bacteria and in turn the biodegradation rates [4,5]. Evaluating and understanding the detachment mechanisms is thus required to better predict the spatial distribution of the microbial population and their associated microbial activities.

* Corresponding author at: Université de Toulouse, INSA, UPS, INP, LISBP, 135 Avenue de Rangueil, F-31077 Toulouse, France. Tel.: +33 561 559 772; fax: +33 561 559 758.

E-mail address: nicolas.derlon@eawag.ch (N. Derlon).

[1] Present address: EAWAG, Ueberlandstrasse 133, P.O. Box 611, 8600 Dübendorf, Switzerland.

[2] Present address: Laboratoire de Génie Chimique, INPT-ENSIACET, 4, allée Emile Monso, BP 44362, 31432 Toulouse Cedex 4, France.

Different mechanisms induce biofilm detachment, e.g, erosion and sloughing [6]. Erosion is a continuous process that affects the entire biofilm surface and detaches small particles [4]. Sloughing is a discrete and local detachment of particles with size similar to the biofilm thickness [4]. Sloughing thus affects the biofilm up to its basis and differs from erosion by its frequency and extent. Despite this size-dependant definition of these two detachment processes, only a little is known about the extent and frequency of erosion and sloughing. The distinction may be arbitrary since a wide range of biofilms can experience with detachment of broad distribution of particles size [6]. However, only few studies aimed at quantifying the extent and frequency of the different detachment mechanisms [1,7]. These studies were in addition either performed on young and thin biofilm [1] or with filtration of the particles that may induce a bias in the measurement [7]. Also, none of these studies aimed at identifying detachment mechanisms with regard of the initial biofilm physical structure, which limit the understanding of the detachment mechanisms.

Erosion and sloughing have been hypothesized to result from a combination of internal biofilm processes and shear and normal forces exerted by moving fluid in contact with the biofilm surface [8]. But the biofilm structure seems to be one of the central determining factors in biofilm detachment [9]. The biofilm physical structure, e.g. the presence of biofilm surface heterogeneities, locally increases the shear stress acting on the biofilm matrix and resulting in detachment [9]. If biofilm detachment mechanisms are influenced by the biofilm physical structures, it is then hypothesized that different biofilm physical structures should be associated with different detachment processes in terms of extent and frequency.

Both hydrodynamic and environmental growth conditions influence the biofilm structure formation [10,11]. An increasing loading rate applied under a stable shear stress induces the formation thicker and rougher biofilms [5,11]. The nature of the electron donor and acceptor also influence the biofilm thickness and its roughness [12,13]. Anoxic biofilms are smoother and thicker biofilms than aerobic biofilm that are characterized by a thin but rough structure. If different biofilm structures develop depending of the environmental growth conditions, it is then hypothesized that detachment properties (extent and frequency) of the corresponding biofilms would be different. A better understanding of the link between the environmental growth conditions (aerobic vs anoxic), the resulting biofilm structure and the detachment properties is thus required.

The main objectives of this study were (i) to quantify the extent and frequency of the detachment processes for different types of biofilms developed under a wide range of environmental conditions and (ii) to link the properties of detachment process with the biofilm physical structures (iii) to better understand how does the potential of bacterial growth in the deep biofilm layers (due to anoxic conditions), influence the biofilm physical structure and in turn the mechanisms of detachment. Biofilms were developed under controlled hydrodynamic conditions in Couette–Taylor reactors. Five biofilms were cultivated under various growth conditions in terms of electron donor, electron terminal acceptor, COD/TKN ratio in order to develop different physical structures. Both the physical properties of the detached particles and of the residual biofilm structures were monitored using light-scattering and image analysis over a long-term period of several months. The detachment mechanisms in terms of extent and frequency were then evaluated with regard of the physical structure of the biofilm.

2. Materials and methods

2.1. Experimental setups for biofilm growth

Biofilms were cultivated in Couette–Taylor Reactors (CTRs) (Fig. 1). The CTR consisted in a pair of concentric cylinders of 200 mm high. The rotating inner cylinder had a radius of 100 mm (R_i). The fixed outer cylinder had a radius of 115 mm. Polyethylene supports for biofilm growth were fixed on the outer cylinder. The hydrodynamic stress was governed by the size/width of the gap between cylinders and by the rotational speed of the inner cylinder. Two different correlations were used to determine the corresponding values of the wall shear stress [14,15]. Low shear stress values of either 0.1 or 0.5 Pa was applied in this study.

Smooth rectangular plastic plates made of Polyethylene were used as substratum for the biofilms. The total surface available for biofilm growth was 0.117 m^2 corresponding to 26 plates. Plates were fixed to the reactor wall using screws. A first peristaltic pump was used to inject the feeding solutions. Silicon tubing was used for the connections. A second peristaltic pump insured the recirculation of the liquid through an aeration chamber. Oxygen concentration higher than 8 mg O_2 L^{-1} was maintained for the growth of biofilm under aerobic conditions. For anoxic growth conditions a cover was kept in contact with the liquid to limit the oxygen transfer and thus maintain an oxygen concentration lower than 0.1 mg O_2 L^{-1} in the bulk liquid. Hydraulic Residence Time (HRT) was 1 day in all experiments. Reactor surfaces and tubing were mechanically cleaned and exchanged, respectively, to avoid biofilm growth outside of the plates.
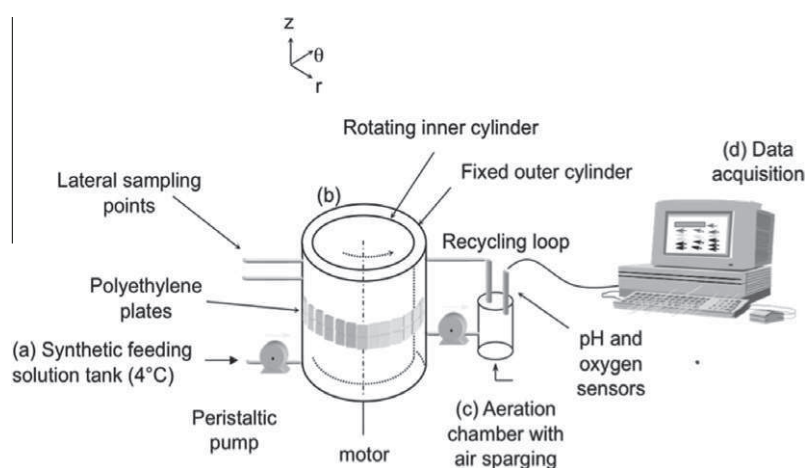

Fig. 1. Experimental setup including (a) the tank filled with the feeding solution, (b) the Couette–Taylor reactor, (c) the aeration chamber with pH and oxygen probes and (d) the data aquisition system.

2.2. Experimental growth conditions

The reactors were inoculated with conventional activated sludge from a laboratory-scale reactor. Five different growth conditions were applied in this study as detailed in Table 1.

The monitoring of the biofilm structure and detachment properties was performed once stable removal efficiencies were observed (in terms of COD removal and nitrification efficiencies). The time needed to reach this steady state slightly changed depending of the growth conditions but was usually close from 45 days. Monitoring of the physical properties of the biofilms and detached particles was performed between days 60 and 120.

2.3. Growth regime characterization and associated measurements

2.3.1. Growth regime characteristic parameters

The use of $\gamma_{S,O2}$ [16] and $\gamma_{S,NO3}$ was introduced to evaluate the growth regime under aerobic and anoxic conditions, respectively:

$$\gamma_{S,O_2} = (1 - Y_{HET,O_2}) \frac{D_S}{D_{O_2}} \frac{S_{S,Lf}}{S_{O_2,Lf}} \tag{1}$$

$$\gamma_{S,NO_3} = \frac{(1 - Y_{HET,NO_3})}{2.86} \frac{D_S}{D_{NO_3}} \frac{S_{S,Lf}}{S_{NO_3,Lf}} \tag{2}$$

In Eqs. 1 and 2, D_S, D_{O2}, and D_{NO3} define the diffusion coefficients for organic substrate, oxygen and nitrates (in $m^2 d^{-1}$). S_S, S_{O2} and S_{NO3} represent their respective concentrations at the biofilm surface (L_f) in g COD m^{-3}, g O_2 m^{-3} and g NO_3^-N m^{-3}, respectively. $Y_{HET,O2}$ and $Y_{HET,NO3}$ define the aerobic and anoxic heterotrophic conversion yields expressed in g CODg O_2^{-1} and in g COD g $NO_3^- -N^{-1}$, respectively.

2.3.2. Analytical methods for the growth regime characterization

Ammonia (NH_4^+), nitrite (NO_2^-), nitrate (NO_3^-) and COD were daily measured in the inlet and in the outlet of the CTRs. The ammonia concentration was measured using the Nessler method (AFNOR, NFT 90.015). Nitrite and Nitrate were measured by spectrometry (AFNOR, NFT 90.012). The COD was measured using test tube reagent sets (Hanna Instruments).

2.4. Detachment processes and associated measurements

Various methods have been developed to characterize the detachment processes. A first approach consists in characterizing the physical structure of the biofilms i.e. its roughness, average and local thicknesses [2,12]. A second approach consists in characterizing the size distribution of the detached particles [1,7]. In this study both the physical structure of the residual biofilms and of the detached particles were quantified to identify the mechanisms of biofilm detachment. Biofilm physical properties were monitored using by image analysis. Detached particles size was monitored using light-scattering.

Table 1
Details of the different growth regimes applied in this study.

Case	Carbon source	Final electron acceptor (in excess)	Organic surface loading rate (g COD $m^{-2} d^{-1}$)	COD/TKN ratio (g COD g N^{-1})
1	Mixed	Oxygen	2.5	73
2	Glucose	Oxygen	38	20
3	Mixed	Oxygen	2.5	4
4	Glucose	Nitrates	38	20
5	Ethanol	Nitrates	38	20

2.4.1. Biofilm morphology, thicknesses and surface roughness

Biofilm physical structure was quantified in terms of morphology, average thickness and surface roughness, based on biofilm pictures. Plates from the biofilm reactor were sampled and placed in a rectangular and transparent plastic box filled with supernatant (centrifuged at 4500g over 15 min). Biofilm side-views images were then captured with a CCD Camera (Kodak Megaplus ES1.0, New York, USA) fitted with a 60 mm Nikon objective. The size of the image was 40×10 mm. The average biofilm thickness and the roughness coefficients (absolute and relative) were then measured using an image analysis program developed with VISILOG 5.4® (NOESIS, Saint-Aubin, France). Two hundred measurements of the local biofilm thickness were performed per image. 20 images of biofilm were recorded and quantified for each growth condition. Average biofilm thickness was defined as the arithmetic mean of the local biofilm thicknesses (200 measurements per images, 20 biofilm images per growth condition). The absolute (R_a) and relative (R_a') roughness were calculated according the following equations:

$$R_a = \frac{1}{n} \sum (|Z_i - \overline{Z}|) \tag{3}$$

$$R_a' = \frac{1}{n} \sum \left(\left| \frac{Z_i - \overline{Z}}{\overline{Z}} \right| \right) \tag{4}$$

where n is the number of measurements, Z_i is the local biofilm thickness (μm) and $\overline{Z}$ is the mean biofilm thickness (μm).

2.4.2. Detached particles size

Detachment process was evaluated by measuring the size of the detached particles using light scattering. Based on these measurements and on the mean biofilm thickness measured by image analysis, the corresponding fraction of the biofilm thickness subjected to detachment was deduced. The procedure was as follow: after each cleaning procedure, the reactors were filled with centrifuged supernatant (centrifugation at 4500g, 15 min) and the rotation of the inner cylinder was started. Meanwhile pumps were switched off to prevent unwanted breakage of the detached particles prior measurements. After 2 h, detached particles were sampled using the tangential outlet of the reactor to avoid modification of their structure (breakage, re-agglomeration) and size-distribution measurements were performed (Mastersizer 2000 Malvern, Worcestershire WR14 1XZ, United Kingdom) (sizes ranged from 0.02 μm to 2000 μm). For this purpose, 800 mL of supernatant containing detached particles were sampled and six light-scattering measurements per sample were performed. During measurement, the samples were gently mixed using a magnetic stirrer. Measurements were performed three times a week between day 60 and day 120, which corresponds to the monitoring of around 150 light-scattering measurement per biofilm. The measured particle sizes were thus representative of that of the detached particles. Number-based distributions are related to the majority-detached particles. Both the $d_{0.5}$ (equivalent diameter of 50% of the detached particles) and the $d_{0.95}$ (equivalent diameter of 95% of the detached particles) were used to estimate the size of the detached particles. The ratio between the $d_{0.5}$ (or $d_{0.95}$) to the average biofilm thickness were calculated to evaluate to what extent detachment impact biofilm thickness.

3. Results

3.1. Growth regime characterization

Microbial functions observed for the five biofilms and the associated nomenclature are detailed in Table 2.

Data from Table 2 confirm that different biofilms in terms of microbial functions developed, i.e., two aerobic Heterotrophic

Table 2
Microbial functions of the biofilms and the associated nomenclature. In the nomenclature, small letters indicate the growth conditions in terms of final electron acceptor: "ae" for aerobic respiration and "an" for anoxic respiration. Bold letters indicate the type of biofilm in terms of microbial functions that were observed: "HB" for Heterotrophic Biofilm and "MAHB" for Mixte Autotrophic and Heterotrophic Biofilm.

Case	Values of $\gamma_{S,O2}$ or $\gamma_{S,NO3}$ coefficients	COD removal efficiency (%)	Nitrification efficiency (%)	Denitrification efficiency (%)	Type of biofilm	Nomenclature
1	0.9	96	0	0	aerobic Heterotrophic Biofilm	aeHB1
2	>1	–	0	0	aerobic Heterotrophic Biofilm	aeHB2
3	0.44	90	85	50	aerobic/anoxic Mixte Autotrophic and Heterotrophic Biofilm	MAHB
4	<1	>90	0	100[a]	anoxic Heterotrophic Biofilm	anHB1
5	<1	>90	0	100[a]	anoxic Heterotrophic Biofilm	anHB2

[a] Due to excess of nitrate and oxygen concentration nil.

Biofilms (aeHB1 and aeHB2), one Mixed Autotrophic and Heterotrophic Biofilm (MAHB) and two anoxic Heterotrophic Biofilms (anHB1 and anHB2). $\gamma_{S,O2}$ coefficients of 0.9 and 0.44 were calculated for aeHB1 and MAHB, respectively. anHB1 and anHB2 were cultivated under excess of final electron acceptor and we assumed $\gamma_{S,NO3}$ coefficients lower than 1 due to the excess of nitrates. A $\gamma_{S,O2}$ coefficient larger than 1 was assumed for aeHB2 due to the oxygen limitation. A partial but high COD removal (>90%) was observed for the biofilms grown under COD limiting conditions (aeHB1, MAHB, anHB1 and anHB2). Nitrification was observed only in the case of the MAHB. A nitrification yield of 85% was monitored that corresponded to a nitrification rate of 0.6 g $NH_4^+ - N$ m^2 d^{-1} for this biofilm. Denitrification was observed for MAHB, anHB1 and anHB2. A significant denitrification efficiency (50%) was surprisingly shown for MAHB despite the excess of oxygen that resulted in the calculation of a $\gamma_{S,O2}$ coefficient of 0.44. But the flux of denitrification remained low $(0.3$ g $NO_3^- - N$ m^{-2} d$^{-1})$ compared to those observed for anHB1 and anHB2 $(> 100$ g $NO_3^- - N$ M^{-2} d^{-1} considering a ratio of 2.86 g $NO_3^- - N$ g $COD^{-1})$. Neither nitrification nor denitrification were observed for aeHB1 (very strong limitation in nitrogen) and aeHB2 (oxygen limitation). The main distinction in terms of microbial functions can thus be done between biofilms grown under aerobic conditions in absence of denitrification (aeHB1 and aeHB2) and those grown under anoxic conditions with denitrification (MAHB, anHB1 and anHB2).

3.2. Biofilm structure monitoring

The different biofilm morphologies that resulted from the different environmental growth conditions are shown in Fig. 2. The mean biofilm thicknesses measured for these biofilms are shown in Fig. 3.

The different environmental growth conditions directly influenced the morphology and physical properties of the biofilms (Figs. 2 and 3). aeHB1 was particularly thick (4400 ± 1100 μm), stringy and fluffy. aeHB2 was also thick (3400 ± 1000 μm) and presents a "finger like" structure composed of numerous streamers. A great amount of filamentous organisms were found in aeHB1 and at a lower degree in aeHB2. Under aerobic conditions and with limitation in oxygen or ammonia, opened and heterogeneous biofilms structures thus developed. On the other hand, the denitrifying biofilms (MAHB, anHB1 and anHB2) were significantly thinner, flatter and more compact than aeHB1 and aeHB2. anHB2 was the smoothest biofilm with a "gel-like" structure. No strict relationship between organic substrate loading rate and resulting biofilm thickness was observed. A decreasing biofilm thickness was however observed for an increasing flux of denitrification.

Absolute and relative roughness coefficients measured for the different types of biofilms are presented in Table 3. Absolute roughness coefficients quantified for denitrifying biofilms were lower than those quantified for non-denitrifying biofilms. A decreasing absolute roughness was thus correlated with an increasing flux of denitrification. However as the mean biofilm thickness also decreased with an increasing flux of denitrification, the relative roughness coefficients were almost similar whatever the microbial functions of the biofilms (around 25%).

3.3. Detached particle characterization

Physical properties of the detached particles were monitored to evaluate the mechanisms of detachment. An example of number-based (Fig. 4A) and volume-based (Fig. 4B) distribution for the detached particles of anHB1 is shown on Fig. 4. A majority of detached particles had a diameter smaller than 2 μm (Fig. 4A).

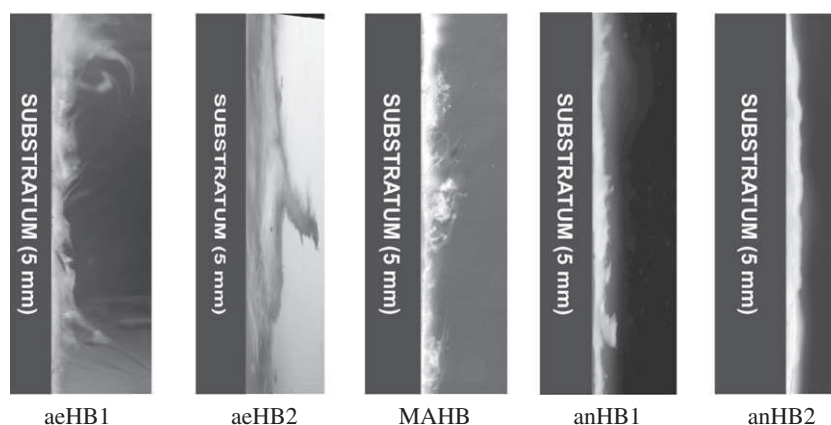aeHB1   aeHB2   MAHB   anHB1   anHB2

Fig. 2. Side-view pictures of the aerobic heterotrophic biofilms (aeHB1 and aeHB2), of the mixed autotrophic heterotrophic biofilms (MAHB) and of the anoxic heterotrophic biofilms (anHB1 and anHB2).
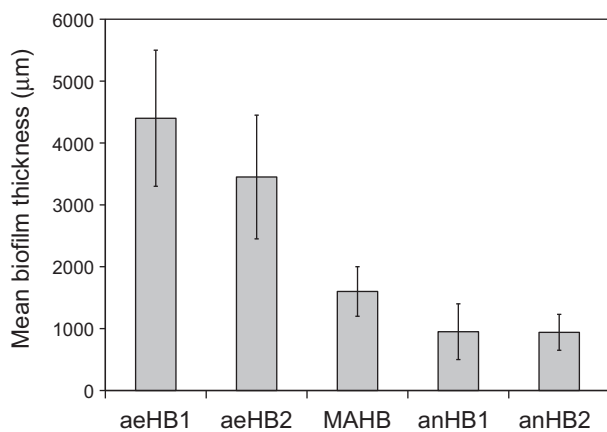
Fig. 3. Mean biofilm thicknesses measured for the aerobic Heterotrophic Biofilms (aeHB1 and aeHB2), the Mixed Autotrophic Heterotrophic Biofilms (MAHB) and the anoxic Heterotrophic Biofilms (anHB1 and anHB2). Bars indicate standard deviations of the mean biofilm thickness ($n = 20$).

Table 3
Absolute and relative roughness coefficients of the aerobic heterotrophic biofilms (aeHB1 and aeHB2), of the mixed autotrophic and heterotrophic biofilm (MAHB) and of the anoxic heterotrophic biofilms (anHB1 and anHB2).

	Non-denitrifying biofilms		Denitrifiying biofilms		
	aeHB1	aeHB2	MAHB	anHB1	anHB2
Absolute roughness coefficient (µm)	1300	900	400	350	250
Relative roughness coefficient (%)	23	25	25	35	26

Detachment of large particles (equivalent diameter ranging from 100 to 200 µm) was also noticed based on the volume-based size distribution (Fig. 4B). This detachment of large particles was observed for each measurement and whatever the type of biofilm.

The ranges of the $d_{0.5}$ calculated from the number (a) and volume-based distributions (b) for the different types of biofilms are shown in Fig. 5. The $d_{0.5}$ of the small particles varied between 1 and 5 µm and between 0.1 and 3 µm for the aeHBs and for the denitrifying biofilms (MAHB and anHBs), respectively (Fig. 5A). The $d_{0.5}$ of the large particles varied from around 30 to 500 µm for the aeHBs and the MAHB. Smaller variations were noticed for the anHBs (ranging from 50 to 90 µm). The ranges of variation of the

$d_{0.5}$ of both small and large particles were thus smaller for the denitrifying biofilms compared with the non-denitrifying biofilms.

A determining point is to evaluate the fraction of biofilm that is impacted by the detachment of the large particles. The ratio between the $d_{0.5}$ (Fig. 6A) or the $d_{0.95}$ (Fig. 6B) and the mean biofilm thickness were calculated for each type of biofilms (Fig. 6). The $d_{0.5}$ and $d_{0.95}$ of volume-based distributions (large particles) were considered for these calculations. The fraction of the mean biofilm thickness impacted by the detachment of large particles varies greatly. In average and with regard of the $d_{0.5}$, up to 25% of the biofilm thickness is regularly impacted by the detachment of large particles (Fig. 6A). Considering the largest particles ($d_{0.95}$), their detachment can impact up to 75% of the mean biofilm thickness (case of the MAHB, Fig. 6B). An influence of the environmental growth conditions is also reported. For aeHB1 and aeHB2, the size of the biofilm heterogeneities (25% in relative roughness coefficients, Table 3) is similar to the fraction of biofilm that is removed due to the detachment of large particles. For MAHB and anHBs, the size of the heterogeneities is smaller than the fraction of biofilm that is removed due to the detachment of large particles.

3.4. Link between the environmental growth conditions, the resulting biofilm structure and the detachment patterns

A summary of the main characteristics of the five different biofilms in terms of morphology, physical properties and detachment patterns is provided in Table 4.

4. Discussion

4.1. How do environmental growth conditions influence microbial functions and in turn the biofilm structure?

Our study highlights the impact of the environmental growth conditions on the biofilm functions and in turn on the physical biofilm structures. With regard of the biofilm physical structure, the influence of the shear conditions, of the mass transfer limitation and of the specific growth rate of the bacteria was reported into the literature. An increasing biofilm heterogeneity results from a decreasing shear stress [10], an increasing mass-transfer limitation [17] or an increasing specific growth rate [4]. In our study we observed the impacts of nitrogen limitation (aeHB1), of oxygen limitation (aeHB2) as well as the impact of the function of denitrification (MAHB, anHB1 and anHB2) on the biofilm physical structure.

Thick and rough biofilms developed under nitrogen (aeHB1) and oxygen-limiting conditions (aeHB2). Limiting environments
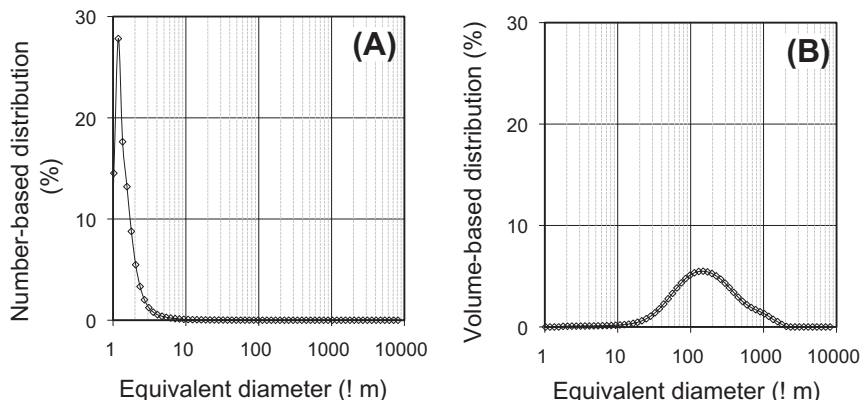

Fig. 4. Examples of number-based (A) and volume based distributions and (B) for anHB1 obtained at steady-state from light-scattering measurement.
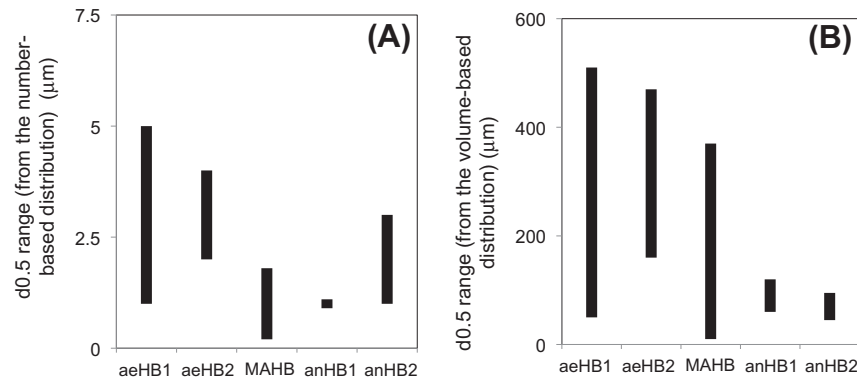
Fig. 5. Ranges of the $d_{0.5}$ (µm) of the five different biofilms, calculated from the number (A) and volume-based (B) distributions. Ranges indicate the variations of all the $d_{0.5}$ values measured during the 2 month measurement period.
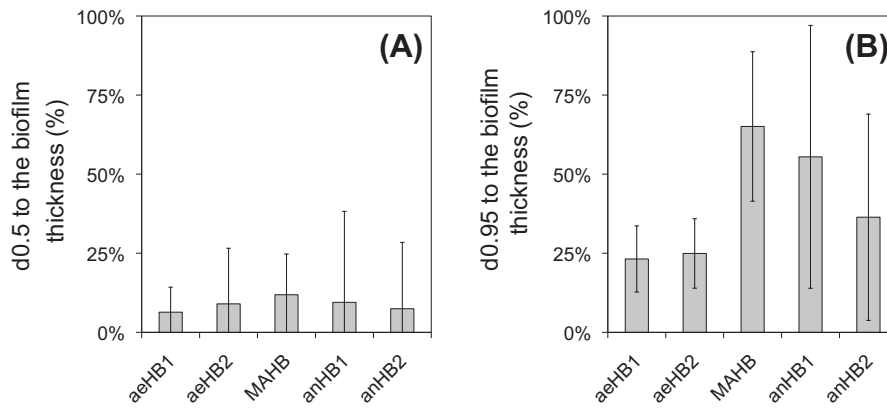

Fig. 6. Ratio between the (A) $d_{0.5}$ and (B) $d_{0.95}$ of the large particles to the biofilm thickness as a function of the type of biofilm. Bars indicate standard deviations calculated from the specific standard deviation of the mean biofilm thickness and of the $d_{0.5}$ or $d_{0.95}$.

Table 4
Summary of the main characteristics of the five different biofilms in terms of morphology, physical properties and detachment patterns.

Biofilm type	Microbial functions	Morphology and physical properties	Detachment patterns
aeHB1 aeHB2	Aerobic heterotrophic	Fluffy, thick and rough (open structure). Significant presence of filamentous bacteria. High absolute roughness coefficient	Large particles detached (up to 500 µm) with significant variations of size over the characterization period. Around 25% of the biofilm thickness was impacted, which corresponded to the relative roughness coefficient
MAHB	Aerobic/anoxic autotrophic heterotrophic	Thin and smooth, with low surface heterogeneities. The smoothness increased with the denitrification potential. Filamentous bacteria are not observed in these three biofilms. Low absolute roughness coefficient	Larges particles detached but a low variation in their size was observed. 25–75% of the biofilm thickness was impacted, which is larger than mean size of the biofilm heterogeneities
anHB1 anHB2	Anoxic heterotrophic		

in terms of substrate availability enhance the tendency of microorganisms to grow toward the bulk liquid [10] which results in the formation of open and heterogeneous biofilm structures. Similar observations were also performed in the case of granules [18] where a decrease in the oxygen availability caused deterioration, decreased density and structure breakage [18]. When decreasing the oxygen or nitrogen availability, we observed that specific microbial populations were selected. A specific microbial ecology with a high fraction of filamentous bacteria developed in aeHB1 and aeHB2. The bacteria that grow as filaments have an enhanced access to the nutrients that are available in the bulk liquid because of their high surface/volume ratio [19]. Filamentous bacteria thus have an ecological advantage compared to conventional bacteria [20]. The shape of the filamentous bacteria favors in turn the devel-

opment of thick biofilm structures. In our study, biofilms developed under substrate limited conditions were 2–4 times thicker than other biofilms, which was mainly due to their high absolute roughness.

Anoxic environments induced in our study the development of smooth and compact biofilms (MAHB, anHB1 and anHB2) suggesting the important role of the function of denitrification on the biofilm physical structure. Similar observations with regard of the influence of the denitrification on the morphology of granular sludge were reported [21]. Highly dense and cauliflower shaped granules developed at high denitrification flux. Fuzzy and porous granules with a rough surface in turn developed at low denitrification flux. When the denitrification flux is increased, bacteria can grow deeper into the biofilm thus reducing growth of fast-growing

bacteria in the top layers. This results in a reduction of the surface heterogeneities [21]. A decrease in the stratification of the microbial populations due to the increase in electron acceptor in the deep biofilm layer thus explain the smooth surface developed by anoxic biofilms. In our study, the increase of the anoxic growth in the deep biofilm layer resulted in a reduction of the absolute biofilm roughness and in turn in the formation of thinner biofilm.

In conclusion, our results confirm that the availability of substrates or nutrient govern the formation of the mesoscale biofilm structure through its influence on the microbial population selection and stratification. When the substrate/nutrient availability is low, bacteria that have an ecological advantage are selected and grow toward the bulk liquid, resulting in the formation of open and heterogeneous structure. When the substrate/nutrient availability is high, bacteria grow deeper into the biofilm, which reduce the formation of heterogeneities and lead the development of flat and compact biofilms.

4.2. What are the mechanisms of biofilm detachment in terms of frequency and extent of detachment event?

The detachment of small and large particles was observed for all types of biofilms independently of their morphology. The detachment of large detached particles was already reported in the literature [1,7]. These studies indeed reported that detachment of small particles (of several microns) dominates the number-based distributions but that the detachment of large particles (several hundreds of microns) dominates the volume-based distributions. But these studies were performed either on young and thin pure culture biofilms [1] or with filtration of the detached particles that may bias the measurements [7], and without considering the physical properties of the biofilms.

Our results confirmed that the detachment of large particles occurred at high frequency and dominated the loss of biomass. Measurements of the detached particles size were indeed performed twice a week and particles of several hundreds of microns were observed for each measurement. The detachment of large particles observed in our study is independent of the biofilm morphology and also, it cannot be associated with sloughing events. Sloughing is indeed a discrete process that is defined as a significant detachment of the biofilm till its basis [6]. Sloughing thus occurs at low frequency and particles detached during sloughing have a size similar to the biofilm thickness. Discrete events that can trigger sloughing of biofilm include a sudden change in the shear stress [5,7] or a change in the availability of oxygen and nutrients [19]. In our study the environmental and hydrodynamic growth conditions were stable over time and thus not explain such a frequent detachment of large particles. Despite the large size of the particles that were detached, the high occurrence of their detachment cannot be attributed to sloughing, which suggests that another mechanism was responsible of their removal.

The detachment of large particles can however be explained by the local interactions between the hydrodynamics and the structural heterogeneities of the biofilms. The development of heterogeneities at the surface of the biofilm induces a modification of the local hydrodynamics in the vicinity of the biofilm/at the biofilm scale [22]. Local shear stress induced by the flow moving through the biofilm heterogeneities can be seven times higher than the global shear [22] leading to the detachment of the biofilm heterogeneities at their basis. In our study, the particles detached from rough aerobic biofilms (aeHBs) were larger than those detached from smooth anoxic biofilms (MAHB and anHBs). This observation was done both for small and large particles (according number-based and volume-based distributions, respectively). Also, the absolute roughness coefficients of the aeHBs were in turn higher than those measured for MAHB and anHBs. An increasing biofilm roughness

thus induces an increasing size of the detached particles. This confirms that the detachment of large particles under constant global shear is probably due to hydrodynamics that act locally on the biofilm heterogeneities. Moreover the frequency of detachment of the biofilm heterogeneities is probably high because of the low cohesion of the top layers of the biofilms, which is independent of the type of biofilm [2].

Overall, the detachment of large particles impacted less than 25% of the mean biofilm thickness (ratio between the $d_{0.5}$ of the large particles to the mean biofilm thickness). But the detachment of very large particles often impacted up to 75% of the mean biofilm thickness (ratio between the $d_{0.95}$ of the large particles to the mean biofilm thickness). The fact that around 20% of the biofilm thickness is never detached is due to the existence of a very cohesive basal layer [2,12] that is never detached even at a shear stress up to 15 Pa.

We can thus conclude that the mechanism of detachment of mature biofilms has two main components. The first component is a surface detachment of small particles of several microns of diameter. The detachment of small particles dominates in number. The second component is the detachment of large particles of several hundreds of microns. This process dominates in volume and is governed by the physical structure of the biofilm in terms of surface roughness and cohesion stratification.

4.3. Implication of the findings in terms of detachment modeling

Different 1-D models can be used to predict biofilm processes [23] and a widely used approach to model biofilm detachment is the surface detachment [5]. Surface detachment implies that the loss of active biomass is determined by the biomass concentration at the biofilm–liquid interface. But our study underlines that the loss of biomass is dominated by volume detachment. The simplifying assumption that detachment is a surface process is probably the cause of numerous deviations observed when using 1-D biofilm models [5]. We suggest that a continuous process of volume detachment should be considered in the detachment models. This would have an impact on the stratification of the microbial populations and thus on the biodegradation rates that requires further investigations.

5. Conclusions

- Continuous erosion of particles of several hundreds of microns of diameter was observed for all types of biofilms.
- Biofilm erosion is composed of a surface process that removes small particles (<20 μm) plus a volume process that removes large particles (<500 μm). Detachment of small particles dominates in number but the detachment of large particles dominates the biomass loss.
- The physical structure of biofilms governs the extent of the volume detachment process. An increasing absolute roughness of the biofilm induces an increase of the size of the large particles that detach.
- An increasing bacterial growth in the deep biofilm layers due to an increasing availability of nitrates induces the formation of thin, smooth and compact biofilm structures.

References

[1] P. Stoodley, S. Wilson, L. Hall-Stoodley, J.D. Boyle, H.M. Lappin-Scott, J.W. Costerton, Growth and detachment of cell clusters from mature mixed-species biofilms, Appl. Environ. Microbiol. 67 (2001) 5608–5613.
[2] N. Derlon, A. Masse, R. Escudie, N. Bernet, E. Paul, Stratification in the cohesion of biofilms grown under various environmental conditions, Water Res. 42 (2008) 2102–2110.

[3] H.C. Flemming, G. Schaule, T. Griebe, J. Schmitt, A. Tamachkiarowa, Biofouling – the Achilles heel of membrane processes, Desalination 113 (1997) 215–225.

[4] E. Morgenroth, P.A. Wilderer, Influence of detachment mechanisms on competition in biofilms, Water Res. 34 (2000) 417–426.

[5] D. Elenter, K. Milferstedt, W. Zhang, M. Hausner, E. Morgenroth, Influence of detachment on substrate removal and microbial ecology in a heterotrophic/autotrophic biofilm, Water Res. 41 (2007) 4657–4671.

[6] P.S. Stewart, A model of biofilm detachment, Biotechnol. Bioeng. 41 (1993) 111–117.

[7] Y.C. Choi, E. Morgenroth, Monitoring biofilm detachment under dynamic changes in shear stress using laser-based particle size analysis and mass fractionation, Water Sci. Technol. 47 (2003) 69–76.

[8] W.G. Characklis, Fouling biofilm development – a process analysis, Biotechnol. Bioeng. 23 (1981) 1923–1960.

[9] M. Bol, R.B. Mohle, M. Haesner, T.R. Neu, H. Horn, R. Krul, 3D finite element model of biofilm detachment using real biofilm structures from CLSM data, Biotechnol. Bioeng. 103 (2009) 177–186.

[10] M.C.M. van Loosdrecht, D. Eikelboom, A. Gjaltema, A. Mulder, L. Tijhuis, J.J. Heijnen, Biofilm structures, Water Sci. Technol. 32 (1995) 35–43.

[11] M.C.M. van Loosdrecht, C. Picioreanu, J.J. Heijnen, A more unifying hypothesis for biofilm structures, FEMS Microbiol. Ecol. 24 (1997) 181–183.

[12] C. Coufort, N. Derlon, J. Ochoa-Chaves, A. Line, E. Paul, Cohesion and detachment in biofilm systems for different electron acceptor and donors, Water Sci. Technol. 55 (2007) 421–428.

[13] A. Ohashi, T. Koyama, K. Syutsubo, H. Harada, A novel method for evaluation of biofilm tensile strength resisting erosion, Water Sci. Technol. 39 (1999) 261–268.

[14] R.J. Donnelly, N.J. Simon, An empirical torque relation for supercritical flow between rotating cylinders, J. Fluid Mech. 7 (1960) 401–418.

[15] F. Wendt, Turbulent Strömungen zwischen zwei rotierenden koaxialen zylindern, Ingen. Arch. A (1933) 577–595.

[16] M. Henze, P. Harremoës, J.L.C. Jansen, E. Arvin, Wastewater Treatment: Biological and Chemical Processes, Springer, Berlin, 1995.

[17] C. Picioreanu, M.C.M. van Loosdrecht, J.J. Heijnen, Effect of diffusive and convective substrate transport on biofilm structure formation: a two-dimensional modeling study, Biotechnol. Bioeng. 69 (2000) 504–515.

[18] A. Mosquera-Corral, M.K. de Kreuk, J.J. Heijnen, M.C.M. van Loosdrecht, Effects of oxygen concentration on N-removal in an aerobic granular sludge reactor, Water Res. 39 (2005) 2676–2686.

[19] K. Garny, T.R. Neu, H. Horn, Sloughing and limited substrate conditions trigger filamentous growth in heterotrophic biofilms – measurements in flow-through tube reactor, Chem. Eng. Sci. 64 (2009) 2723–2732.

[20] A.M.P. Martins, K. Pagilla, J.J. Heijnen, M.C.M. van Loosdrecht, Filamentous bulking sludge – a critical review, Water Res. 38 (2004) 793–817.

[21] J.F. Wan, M. Sperandio, Possible role of denitrification on aerobic granular sludge formation in sequencing batch reactor, Chemosphere 75 (2009) 220–227.

[22] M. Wagner, B. Manz, F. Volke, T.R. Neu, H. Horn, Online assessment of biofilm development, sloughing and forced detachment in tube reactor by means of magnetic resonance microscopy, Biotechnol. Bioeng. 107 (2010) 172–181.

[23] O. Wanner, H. Eberl, E. Morgenroth, D. Noguera, C. Picioreanu, B. Rittmann, M.C.M. van Loosdrecht, Mathematical Modelling of Biofilms, IWA Scientific and Technical Report No.18, IWA Publishing, (ISBN: 1843390876), 2006.